BIRD'S-EYE VISUALIZATION OF DESIGN-KNOWLEDGE DIVERSITY FOR LAUNCH VEHICLE IN VIEW OF FUELS ON HYBRID ROCKET ENGINE

Kazuhisa Chiba[1], Masahiro Kanazaki[2], Masaki Nakamiya[3], Koki Kitagawa[4] and Toru Shimada[4]

[1] Graduate School of Engineering
Hokkaido University of Science
7-15-4-1, Maeda, Teine, Sapporo 006-8585, Japan
e-mail: kazchiba@hus.ac.jp, web page: http://www.geocities.jp/thousandleaf_k/

[2] Graduate School of System Design
Tokyo Metropolitan University
6-6, Asahigaoka, Hino, Tokyo 191-0065, Japan
e-mail: kana@tmu.ac.jp, web page: http://www.comp.sd.tmu.ac.jp/aerodesign/eng.htm

[3] Research Institute for Sustainable Humanosphere
Kyoto University
Gokashou, Uji, Kyoto 611-0011, Japan
e-mail: masaki_nakamiya@rish.kyoto-u.ac.jp

[4] Institute of Space and Astronautical Science
Japan Aerospace Exploration Agency
3-1-1, Yoshinodai, Chuo, Sagamihara 252-5210, Japan
e-mail: {kitagawa.koki, shimada.toru}@jaxa.jp

Key words: Design Informatics, Single-Stage Launch Vehicle for Scientific Observation, Hybrid Rocket Engine Using Solid Fuel and Liquid Oxidizer.

Abstract. A single-stage launch vehicle with hybrid rocket engine, which uses solid fuel and liquid oxidizer, has been being studied and developed as a next-generation rocket for scientific observation due to the advantages as low cost, safety, re-ignition, and reducing pollution. Thereupon, the knowledge regarding hybrid rocket system has been being gained through the forepart of the conceptual design using design informatics. In the present study, the practical problem defined by using three objective functions and seven design variables for aurora observation is treated so as to contribute the real world using evolutionary computation and data mining for the field of aerospace engineering. The primary objective of the design in the present study is that the down range and the duration time in the lower thermosphere are sufficiently obtained for the aurora scientific observation, whereas the initial gross weight is held down. Investigated solid fuels are five,

while liquid oxidizer is considered as liquid oxygen. The condition of single-time ignition is assumed in flight sequence in order to quantitatively investigate the ascendancy of multi-time ignition. A hybrid evolutionary computation between the differential evolution and the genetic algorithm is employed for the multidisciplinary design optimization. A self-organizing map is used for the data mining technique in order to extract global design information. Consequently, the design information regarding the tradeoffs among the objective functions, the behaviors of the design variables in the design space to become the nondominated solutions, and the implication of the design variables for the objective functions have been obtained in order to quantitatively differentiate the advantage of hybrid rocket engine in view of the five fuels. Moreover, the next assignments were also revealed.

1 INTRODUCTION

Single-stage rockets have been being researched and developed for the scientific observations and the experiments of high-altitude zero-gravity condition, whereas multi-stage rockets have been being also studied for the orbit injection of payload. The Institute of Space and Astronautical Science (ISAS), Japan Aerospace Exploration Agency (JAXA) has been operating K(Kappa), L(Lambda), and M(Mu) series rockets as the representatives of solid rocket in order to contribute to the space scientific research. A lower-cost and more efficient rocket is necessary due to the retirement of M-V in 2008 and in order to promote space scientific research. In fact, E(Epsilon) rocket began to be operated from August 2013. On the other hand, the launch vehicle with hybrid rocket engine using solid fuel and liquid oxidizer has been being researched and developed as an innovative technology in mainly Europe and United States[1, 2]. The present study will investigate the conceptual design in order to develop a next-generation single-stage launch vehicle with hybrid rocket engine. Final system for science missions is a multi-stage hybrid rocket in place of E rocket. Single-stage hybrid rocket has a role of technical demonstration for multi-stage one. Since the technologies of hybrid rocket engine for single-stage and multi-stage are not independent, the solution of the fundamental physics regarding single-stage hybrid rocket can be diverted to multi-stage one. A hybrid rocket offers the several advantages as higher safety, lower cost, and pollution free flight. The multi-time ignition is the especial ascendancy of hybrid rocket engine[3]. On the other hand, the disadvantage of a hybrid rocket engine is in its combustion. As a hybrid rocket engine has low regression rate of solid fuel due to turbulent boundary layer combustion, the thrust of hybrid rocket engine is less than that of pure solid and pure liquid engines which can obtain premixed combustion[4]. In addition, as the mixture ratio between solid fuel and liquid oxidizer is temporally fluctuated, thrust becomes unstable. Multidisciplinary design requirements should be considered in order to surmount the disadvantage of hybrid rocket engine. Moreover, exhaustive design information will be obtained in order to additionally

consider productive and market factors(it is difficult that optimization deals with them due to the difficulty of the definition of practical problems).

Design informatics is essential for practical design problems. Although solving design optimization problems is important under the consideration of many disciplines of engineering[5], the most significant part of the process is the extraction of useful knowledge of the design space from results of optimization runs. The results produced by multiobjective optimization (MOO) are not an individual optimal solution but rather an entire set of optimal solutions due to tradeoffs. That is, the result of a MOO is not sufficient from the practical point of view as designers need a conclusive shape and not the entire selection of possible optimal shapes. On the other hand, this set of optimal solutions produced by an evolutionary MOO algorithm can be considered a hypothetical design database for design space. Then, data mining techniques can be applied to this hypothetical database in order to acquire not only useful design knowledge but also the structurization and visualization of design space for the conception support of basic design. This approach was suggested as design informatics[6]. The goal of this approach is the conception support for designers in order to materialize innovation. This methodology is constructed by the three essences as 1) problem definition, 2) efficient optimization, and 3) structurization and visualization of design space by data mining. A design problem including objective function, design variable, and constraint, is strictly defined in view of the background physics for several months(problem definition is the most important process because it directly gives effect on the quality of design space. Since the garrulous objective-function/design-variable space including physics and design information which is not inherently necessary to consider should be performed unnecessary evolutionary exploration and mining, it is conceived to be low-quality design space), then optimization is implemented in order to acquire nondominated solutions (quasi-Pareto solutions) as hypothetical database. Data mining is performed for this database in order to obtain design information. Mining has the role of a postprocess for optimization. Mining result is the significant observations for next design phase and also becomes the material to redefine a design problem.

In the present study, a single-stage launch vehicle with hybrid rocket engine using solid fuel and liquid oxidizer for the scientific observation of aurora will be conceptually designed by using design informatics approach. Finally, the advantage of re-ignition in the science mission for aurora observation will be quantitatively revealed. Moreover, the fundamental physics to achieve a hybrid rocket engine under the combustion mode considered in the present study. As a first step, an optimization problem on single-time ignition, which is the identical condition of the current solid rocket, was defined under the present studying constructions so as to obtain the design information[7]. As a second step, the implication of solid fuels in performance of hybrid rocket will be revealed because the regression rate is one of the key elements for the performance of hybrid rocket. This study corresponds to the above second step. Finally, the sequence using multi-time ignition, which is the advantage of hybrid rocket, will be investigated in order to reveal the

ascendancy of hybrid rocket for aurora observation. This study is a milestone to observe the quantitative difference of performance regarding ignition time.

2   DESIGN INFORMATICS

Design informatics after the definition of detailed problem is constructed by two phases as optimization and data mining. Evolutionary computation is used for optimization. Although a surrogate model[8] like as the Kriging model[9], which is a response surface model developed in the field of spatial statistics and geostatistics, can be employed as optimization method, it will not be selected because it is difficult to deal with a large number of design variables. In addition, since the designers require to present many exact optimum solutions for the decision of a compromise one, an evolutionary-based Pareto approach as an efficient multi-thread algorithm, which the plural individuals are parallel conducted, is employed instead of gradient-based methods. The optimizer used in the present study is the evolutionary hybrid method between the differential evolution (DE) and the genetic algorithm (GA)[10]. Moreover, global design information is primarily essential in order to determine a compromise solution. Therefore, a self-organizing map (SOM)[11, 12] is used as a data mining technique in the present study because SOM extracts the global information in design space[13]. The view of hybridization is inspired by the evolutionary developmental biology[14]. When there is the evolution which the Darwinism cannot explain in the identical species, each individual might have a different evolutionary methodology. When the practical evolution is imitated for the evolutionary computation, the different evolutionary algorithms might ultimately be applied to each individual in population. The making performance of next generation for each methodology depends on not only their algorithms but also the quality of candidate of parent in the archive of nondominated solutions. The present hybridization is intended to improve the quality of candidate of parent by sharing the nondominated solutions in the archive among each methodology. In the present study, the evolutionary hybrid optimization methodology between DE and GA is employed. It was confirmed that this methodology had the high performance regarding the convergence and diversity, as well as the strength for noise[10]. Note that noise imitates the error on computational analyses and experiments and is described as the perturbation on objective functions. It is an important factor when the optimization for practical engineering problem is considered.

First, multiple individuals are generated randomly as an initial population. Then, objective functions are evaluated for each individual. The population size is equally divided into sub-populations between DE and GA (although sub-population size can be changed at every generations on the optimizer, the determined initial sub-populations are fixed at all generations in the present study). New individuals generated by each operation are combined in next generation. The nondominated solutions in the combined population are archived in common. It is notable that only the archive data is in common between DE and GA. The respective optimization methods are independently performed in the present hybrid methodology.

2.1 Configurations of Operators for Each Optimizer

The present optimization methodology is a real-coded optimizer[15]. Although GA is based on the real-coded NSGA-II(the elitist nondominated sorting genetic algorithm)[16], it is made several improvements on in order to be progressed with the diversity of solutions. Fonseca's Pareto ranking[17] and the crowding distance[16] are used for the fitness value of each individual. The stochastic universal sampling[18] is employed for parents selection. The crossover rate is 100%. The principal component analysis blended crossover-α(PCABLX)[19] and the confidence interval based crossover using L_2 norm(CIX)[20] are used because of the high performance for the convergence and the diversity as well as the strength for noise[10]. The subpopulation size served by GA is equally divided for these two crossovers. The mutation rate is set to be constant as the reciprocal of the number of design variables. For alternation of generations, the Best-N selection[16] is used. DE is used as the revised scheme[21] for multiobjective optimization from DE/rand/1/bin scheme. The scaling factor F is set to be 0.5. The present optimizer has the function of range adaptation[22], which changes the search region according to the statistics of better solutions, for all design variables. In the present study, the range adaptation is implemented at every 20th generations.

2.2 Data-Mining Technique

In the present study, SOM is selected as a data-mining technique because the primary objective of data mining is the acquisition of global design information in order to implement the structuring of design space. The previous study[13] indicated that SOM extracted the global design information for whole design space. The distinguishing feature of SOM is the generation of a qualitative description. The advantage of this method includes the intuitive visualization of two-dimensional colored maps of design space using bird's-eye-views. As a result, SOM reveals the tradeoffs among objective functions. Moreover, SOM addresses the effective design variables and also reveals how a specific design variable gives effects on objective functions and other design characteristics. One SOM is colored for one variable of objective function, design variable, and other characteristic value so that the coloring pattern is compared each other. Therefore, the data mining using SOM might have a disadvantage to overlook important correlation in the problem with a large number of objective functions and design variables. Since the present study has a total number of 10 at most among the objective functions and design variables, SOM is sufficient for the data mining manner. In the present study, SOMs are generated by using commercial software Viscovery$^{\circledR}$ SOMine 4.0 plus produced by Eudaptics, GmbH. The uniqueness of the map generated by SOMine is assured due to Kohonen's Batch SOM algorithm and search of the best-matching unit for all input data and adjustment of weight vector near the best-matching unit.

3 Problem Definition

The conceptual design for a single-stage hybrid rocket[23], simply composed of a payload chamber, an oxidizer tank, a combustion chamber, and a nozzle, is considered in the present study. A single-stage hybrid rocket for aurora scientific observation will be focused because the rocket for more efficient scientific observation is desired for successfully obtaining new scientific knowledge on the aurora observation by ISAS in 2009. In addition, a single-stage hybrid rocket problem fits for the resolution of the fundamental physics regarding hybrid rocket engine and for the improvement of the present design problem due to its simplification.

3.1 Objective Functions

Three objective functions are defined in the present study. First objective is the maximization of the down range in the lower thermosphere (altitude of 90 to 150km) R_d [km] (obj1). Second is the maximization of the duration time in the lower thermosphere T_d [sec] (obj2). It recently turns out that atmosphere has furious and intricate motion in the lower thermosphere due to the energy injection, which leads aurora, from high altitude. The view of these objective functions are to secure the horizontal distance and time for the competent observation of atmospheric temperature and the wind for the elucidation of atmospheric dynamics and the balance of thermal energy. Third objective is the minimization of the initial gross weight of launch vehicle $M_{tot}(0)$ [kg] (obj3), which is generally the primary proposition for space transportation system.

3.2 Design Variables

Seven design variables are used as initial mass flow of oxidizer $\dot{m}_{oxi}(0)$ [kg/sec] (dv1), fuel length L_{fuel} [m] (dv2), initial radius of port $r_{port}(0)$ [m] (dv3), combustion time t_{burn} [sec] (dv4), initial pressure in combustion chamber $P_{cc}(0)$ [MPa] (dv5), aperture ratio of nozzle ϵ [-] (dv6), and elevation at launch time ϕ [deg] (dv7). Note that there is no constraint except the limitations of upper/lower values of each design variable summarized in Table 1. These upper/lower values are exhaustively covering the region of design space which is physically admitted. When there is a sweet spot (the region that all objective functions proceed optimum directions) in the objective-function space, the exploration space would intentionally become narrow due to the operation of range adaptation on the evolutionary computation.

6

Table 1: Limitation of upper/lower values of each design variable.

serial number	design variable	design space		
dv1	initial mass flow of oxidizer	$1.0 \leq$	$\dot{m}_{\mathrm{oxi}}(0)$ [kg/sec]	≤ 30.0
dv2	fuel length	$1.0 \leq$	L_{fuel} [m]	≤ 10.0
dv3	initial radius of port	$0.01 \leq$	$r_{\mathrm{port}}(0)$ [m]	≤ 0.30
dv4	combustion time	$10.0 \leq$	t_{burn} [sec]	≤ 40.0
dv5	initial pressure in combustion chamber	$3.0 \leq$	$P_{\mathrm{cc}}(0)$ [MPa]	≤ 6.0
dv6	aperture ratio of nozzle	$5.0 \leq$	ϵ [-]	≤ 8.0
dv7	elevation at launch time	$50.0 \leq$	$\phi(0)$ [deg]	≤ 90.0

3.3 Evaluation Method

First of all, the mixture ratio between liquid oxidizer and solid fuel $O/F(t)$ is computed by the following equation.

$$O/F(t) = \frac{\dot{m}_{\mathrm{oxi}}(t)}{\dot{m}_{\mathrm{fuel}}(t)}.$$
$$\dot{m}_{\mathrm{fuel}}(t) = 2\pi r_{\mathrm{port}}(t) L_{\mathrm{fuel}} \rho_{\mathrm{fuel}} \bar{\dot{r}}_{\mathrm{port}}(t), \tag{1}$$
$$r_{\mathrm{port}}(t) = r_{\mathrm{port}}(0) + \int \dot{r}_{\mathrm{port}}(t) dt.$$

$\dot{m}_{\mathrm{oxi}}(t)$ and $\dot{m}_{\mathrm{fuel}}(t)$ are the mass flow of oxidizer [kg/sec] and the mass flow of fuel [kg/sec] at time t, respectively. $r_{\mathrm{port}}(t)$ is the radius of port [m] at t, L_{fuel} describes fuel length, and ρ_{fuel} is the density of fuel [kg/m^3]. $\dot{r}_{\mathrm{port}}(t)$ describes the regression rate. After that, an analysis of chemical equilibrium is performed by using NASA-CEA (chemical equilibrium with applications) [24], then trajectory, thrust, aerodynamic, and structural analyses are respectively implemented. The present rocket is assumed as a point mass. As the time step is set to be 0.5[sec] in the present study, it takes roughly 10[sec] for the evaluation of an individual using a general desktop computer.

A combustion chamber is filled with solid fuel with a single port at the center to supply oxidizer. As the regression rate to the radial direction of the fuel $\dot{r}_{\mathrm{port}}(t)$ [m/sec] generally governs the thrust power of hybrid rocket engine, it is a significant parameter. The following experimental model[25, 26] is used in the present study.

$$\dot{r}_{\mathrm{port}}(t) = a_{\mathrm{fuel}} \times G_{\mathrm{oxi}}^{n_{\mathrm{fuel}}}(t)$$
$$= a_{\mathrm{fuel}} \times \left(\frac{\dot{m}_{\mathrm{oxi}}(t)}{\pi r_{\mathrm{port}}^2(t)} \right)^{n_{\mathrm{fuel}}}, \tag{2}$$

where, $G_{\mathrm{oxi}}(t)$ is oxidizer mass flux [kg/m^2/sec]. a_{fuel} [m/sec] and n_{fuel} [-] are the constant values experimentally determined by fuels. In the present study, liquid oxygen as liquid oxidizer and five solid fuels are used as thermoplastic resin polypropylene (PP), two WAX-type fuels (FT0070 and PW120), and two compounds between glycidyl azide polymer

Table 2: Characteristic values of the fuels.

fuels	a_{fuel} [mm/sec]	n_{fuel} [-]	density [kg/m^3]
polypropylene	0.0826	0.5500	910.0
WAX FT0070	0.1561	0.3905	926.6
WAX PW120	0.1677	0.4352	896.8
GAP50PEG50	0.3218	0.2937	1180.0
GAP60PEG40	0.4641	0.2864	1196.0
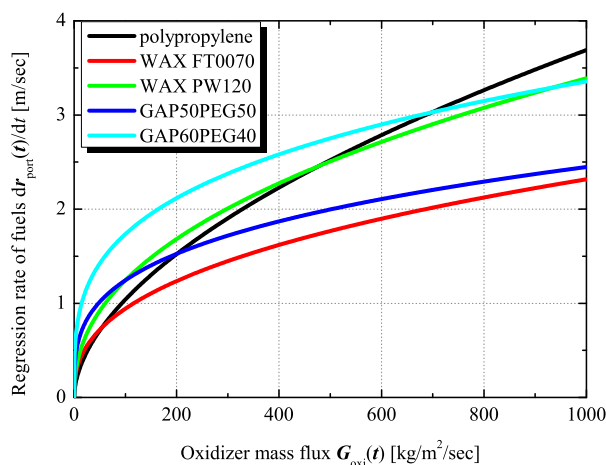
Figure 1: Comparison of the regression rate $\dot{r}_{\mathrm{port}}(t)$ for the oxidizer mass flux $G_{\mathrm{oxi}}(t)$ per unit volume among the fuels.

and polyethylene glycol (GAP50PEG50 and GAP60PEG40, the number means the blend proportion) for solid fuel in order to compare the implications of fuels in the performance of hybrid rocket. Polypropylene has swirling flow for the supply mode of oxidizer and the other fuels have steady flow. The characteristic values of the fuels are summarized in Table 2. The variation of the regression rate $\dot{r}_{\mathrm{port}}(t)$ for the oxidizer mass flux $G_{\mathrm{oxi}}(t)$ represented by eq. (2) is shown in Fig. 1. The regression rate $\dot{r}_{\mathrm{port}}(t)$ of GAP60PEG40 is highest at low $G_{\mathrm{oxi}}(t)$, and $\dot{r}_{\mathrm{port}}(t)$ of WAX FT0070 and GAP50PEG50 is low on the whole.

4 Results

4.1 Optimization Result

The present population size is set to be 18 and evolutionary computation is performed until 3,000 generations. Note that the dependency of the optimization method was firstly investigated using the case of polypropylene. Hypervolume indicator showed that there is no dependency regarding initial populations at 10^3 order of generation. In addition,
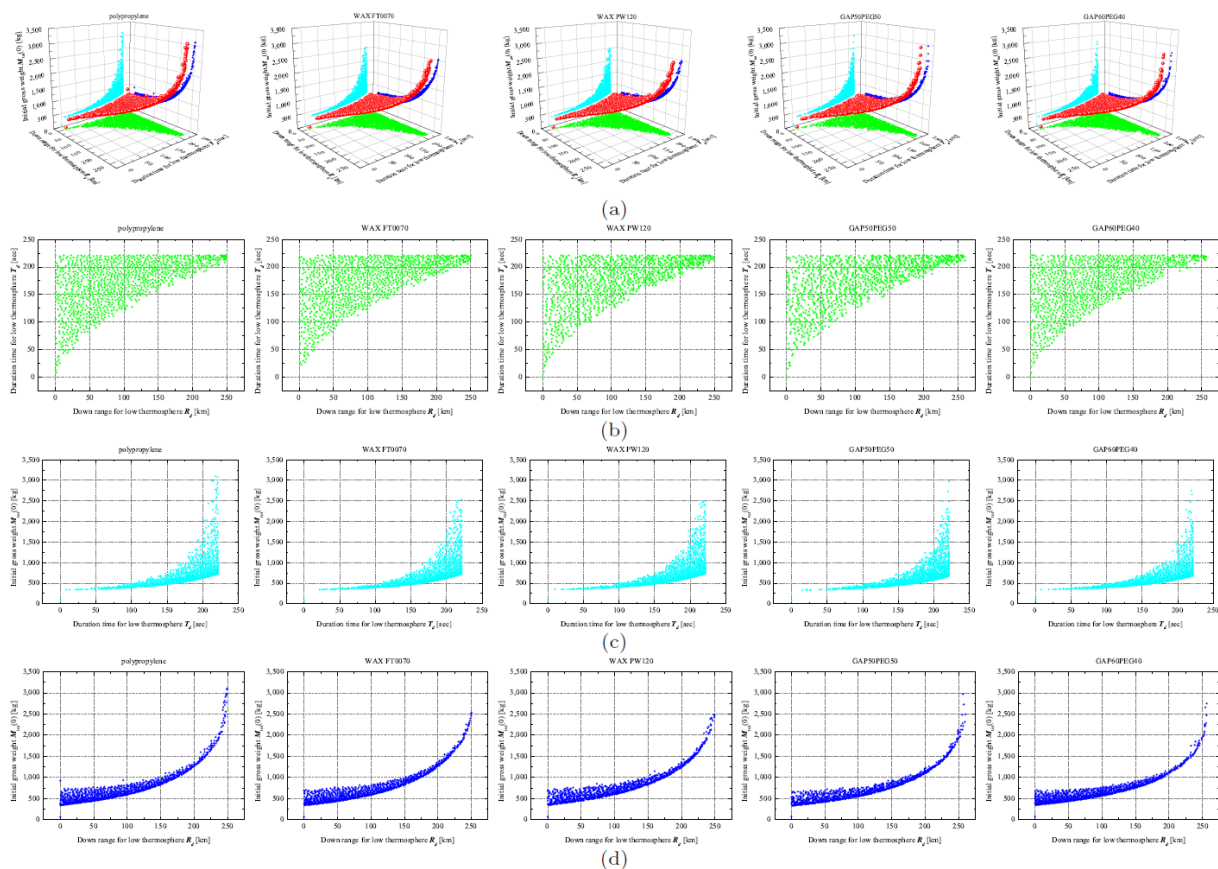
Figure 2: Plots of nondominated solutions on the objective function space, (a) plots in three-dimensional objective function space, (b) two-dimensional plots between the down range R_d(obj1) and the duration time T_d(obj2), (c) two-dimensional plots between the duration time T_d(obj2) and the initial gross weight $M_{\text{tot}}(0)$(obj3), and (d) two-dimensional plots between the down range R_d(obj1) and the initial gross weight $M_{\text{tot}}(0)$(obj3). The column means the results for polypropylene, WAX FT0070, WAX PW120, GAP50PEG50, GAP60PEG40 from the left.

3000 generations have the sufficient convergence of this optimization. Thereupon, the differences among the following optimization results depend on the fuels. The plots of acquired nondominated solutions are shown in Fig. 2. Figure 2(a) is the nondominated solutions in the three-dimensional objective-function space and Figs. 2(b), (c), and (d) are projected onto two-dimensional surfaces in order to intuitively observe the tradeoffs. Figure 2 also reveals that there is no meaningful difference among the fuels for the tendency regarding the correlation among the objective functions. Thereupon, the tradeoffs regarding polypropylene will be observed as a representation.

Figure 2(a) reveals that there generates the connecting and convex nondominated surface except several isolated individuals. There is no tradeoff between the down range R_d and the duration time T_d in the lower thermosphere shown in Fig. 2(b). This figure also shows that there are upper limitations of roughly 250[km] for the down range R_d and

9

220[sec] for the duration time T_d. Therefore, the projection plots onto two dimensions between the down range R_d and the duration time T_d do not converge in one point. In the present study, the initial mass flow of oxidizer $\dot{m}_{\text{oxi}}(0)$ (dv1) has the limitation of upper/lower values. Since the regression rate to the radial direction of the fuel $\dot{r}_{\text{port}}(t)$ as an experimental model uses the mass flow of oxidizer $\dot{m}_{\text{oxi}}(t)$, $\dot{r}_{\text{port}}(t)$ has constraint. As a result, the limitations are generated for the down range R_d and the duration time T_d.

There is an incomplete tradeoff between the duration time T_d and the initial gross weight $M_{\text{tot}}(0)$ shown in Fig. 2(c). The convex nondominated surface to optimum direction with incompleteness is generated due to the limitation of the duration time T_d. As the inclination $dM_{\text{tot}}(0)/dT_d$ is small on the convex curve, the duration time T_d can be substantially improved when trifling initial gross weight $M_{\text{tot}}(0)$ would be sacrificed. In addition, Fig. 2(c) shows that the minimum initial gross weight to reach the limitation of the duration time(roughly 220[sec]) is approximately 700[kg]. And also, the smallest initial gross weight to attain to the lower thermosphere(altitude of 90[km]) is approximately 350[kg]. As these values are better than those of the solid rockets which are operated at present for scientific observation, it suggests that hybrid rocket has an advantage even when hybrid rocket does not have a sequence of multi-time ignition.

There is a severe tradeoff between the down range R_d and the initial gross weight $M_{\text{tot}}(0)$ shown in Fig. 2(d) (although the down range strictly has the upper limitation, it seems that the clean convex curve is generated because the limitation is on the edge of the nondominated surface). This figure shows that the maximum down range is roughly 130[km] when the minimum initial gross weight to reach the limitation of the duration time T_d(approximately 700[kg]) is adopted. The initial gross weight $M_{\text{tot}}(0)$ should be absolutely increased in order to have more down range R_d(greater than 130[km]) despite no increase of the duration time T_d(remaining roughly 220[sec]). This fact suggests that the design strategies for the maximizations of the down range R_d and the duration time T_d are different.

4.2 Data-Mining Result

Figure 3 shows SOMs colored by the objective functions. Figures 4 and 5 show SOMs colored by the design variables. As this SOM learning is implicated based on the values of the objective functions as the indicator for the similarity on the neural network, SOMs colored by the objective functions have absolutely gradation shown in Fig. 3. Generally, as the SOM colored by objective function with gradation can indicate optimum and pessimum directions on SOM, they can be compared. In addition, the directions of influence of design variables for objective functions can be visualized by colored SOMs. This knowledge cannot be revealed by the plots as Fig. 2. This is one of the ascendancy of SOM due to the bird's-eye visualizationn manner on 2-dimensional map. The upper/lower values of coloring range in Fig. 4 are set to be the upper/lower values of each design variable defined in the problem summarized in Table 1. The upper/lower values of coloring range in Fig. 5 is set to be maximum/minimum values of each design variable in nondominated
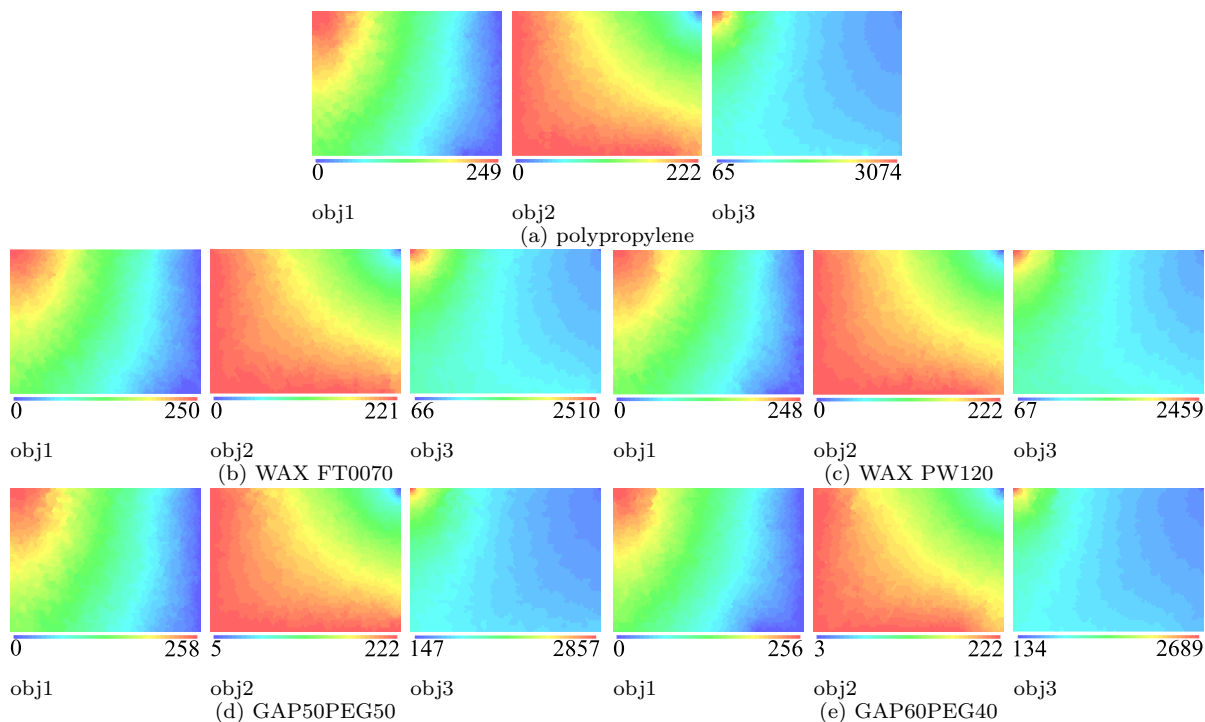
10

Figure 3: SOMs colored by the objective functions.

solutions. Since the evolutionary exploration is performed for the design space, the range for the respective design variables in Fig. 5 becomes absolutely narrow compared with Fig. 4. When the coloration pattern among fuels will be compared on Fig. 3, the qualitative tendency is identical. When the coloration pattern among fuels will be also compared on Figs. 4 and 5, the qualitative tendency is similar although the values themselves have diversity. Thereupon, the qualitative inclination will be described in this section. The implication of fuels is expounded in the next section.

4.2.1   Relationship among Objective Functions

The comparison of the coloring pattern in Fig. 3 reveals the tradeoffs among the objective functions. The coloring patterns of all objective functions are identical among the five fuels. When obj1 is high value (red region), obj2 absolutely becomes high. However, as obj1 does not always become high whenever obj2 is high, this relationship is irreversible. This is because not only the down range R_d (obj1) but also the attained maximum altitude gives the effect on the duration time T_d (obj2). In contrast, when obj2 is low value (blue region), obj1 absolutely becomes low. However, as obj2 does not always become low whenever obj1 is low, this relationship is similarly irreversible. Although there is no tradeoff in the global space of the objective functions, there is locally tradeoff at the right bottom of Fig. 3. This local tradeoff is caused by the limitation of the duration time
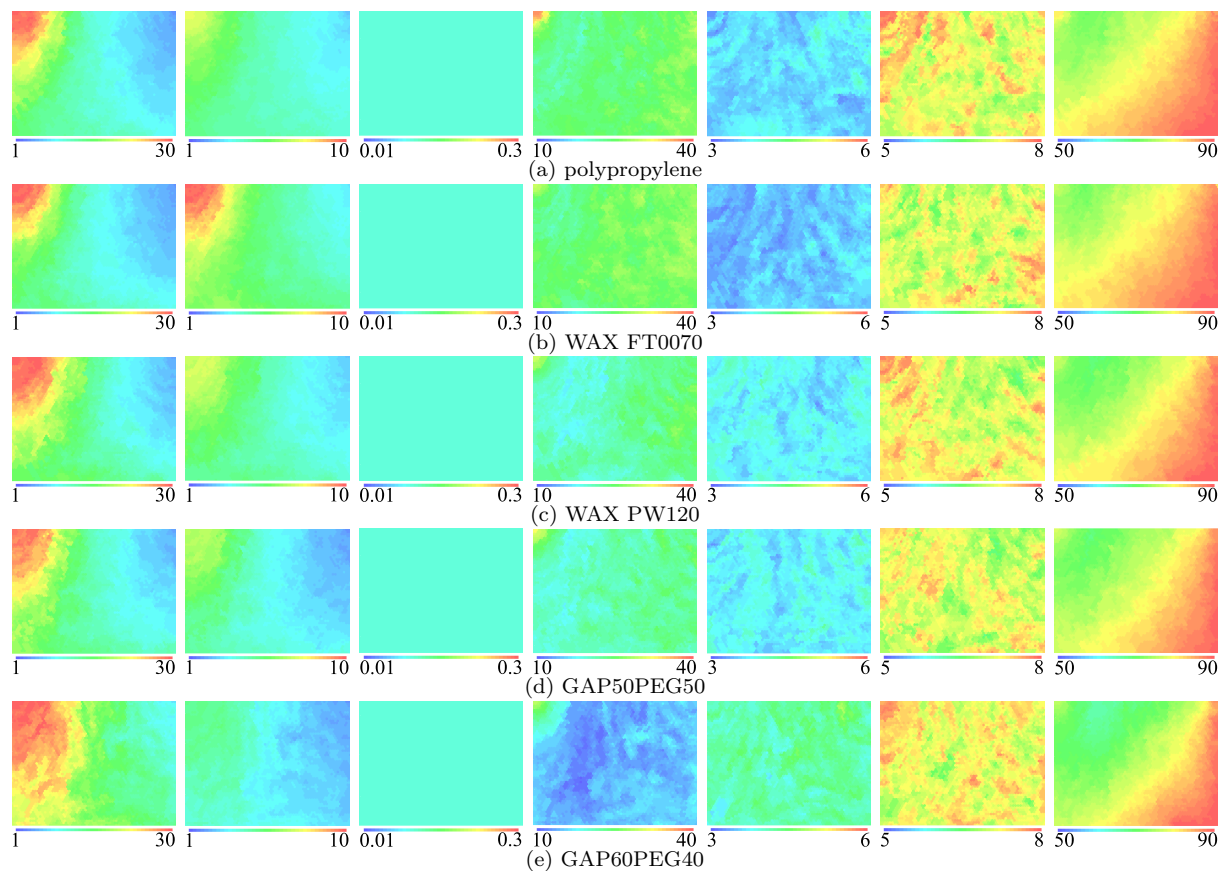
11

Figure 4: SOMs colored by the design variables. The color range is set to be their upper/lower values in the problem definition in Table 1. The column means dv1, dv2, $\cdots$, and dv7 from the left.

T_d(obj2), that is, reaching the maximum value of the duration time T_d(obj2) is easier than achieving the maximum value of the down range R_d(obj1).

Since the initial gross weight $M_{\text{tot}}(0)$(obj3) is the minimization function, there are severe tradeoffs among obj3 and the others. It especially reveals the severe problem that the optimum direction of the down range R_d(obj1) and the pessimum direction of the initial gross weight $M_{\text{tot}}(0)$(obj3) accord(observing the upper left on SOM regarding obj1 and obj2 reveals that the better obj1 and the worse obj3 accord). The structural constraints and the combustion mode should be reconsidered in order to avoid this problem. On the other hand, the optimum region of the duration time T_d(obj2) and the pessimum direction of the initial gross weight $M_{\text{tot}}(0)$(obj3) overlap only in part. Therefore, the initial gross weight $M_{\text{tot}}(0)$ can become low when the duration time T_d is the primary objective. On the other hand, the minimum initial gross weight is decided by the expected down range when the down range R_d is the primary objective, that is, the minimum initial gross weight depends on the mission requirement as the necessary down range.
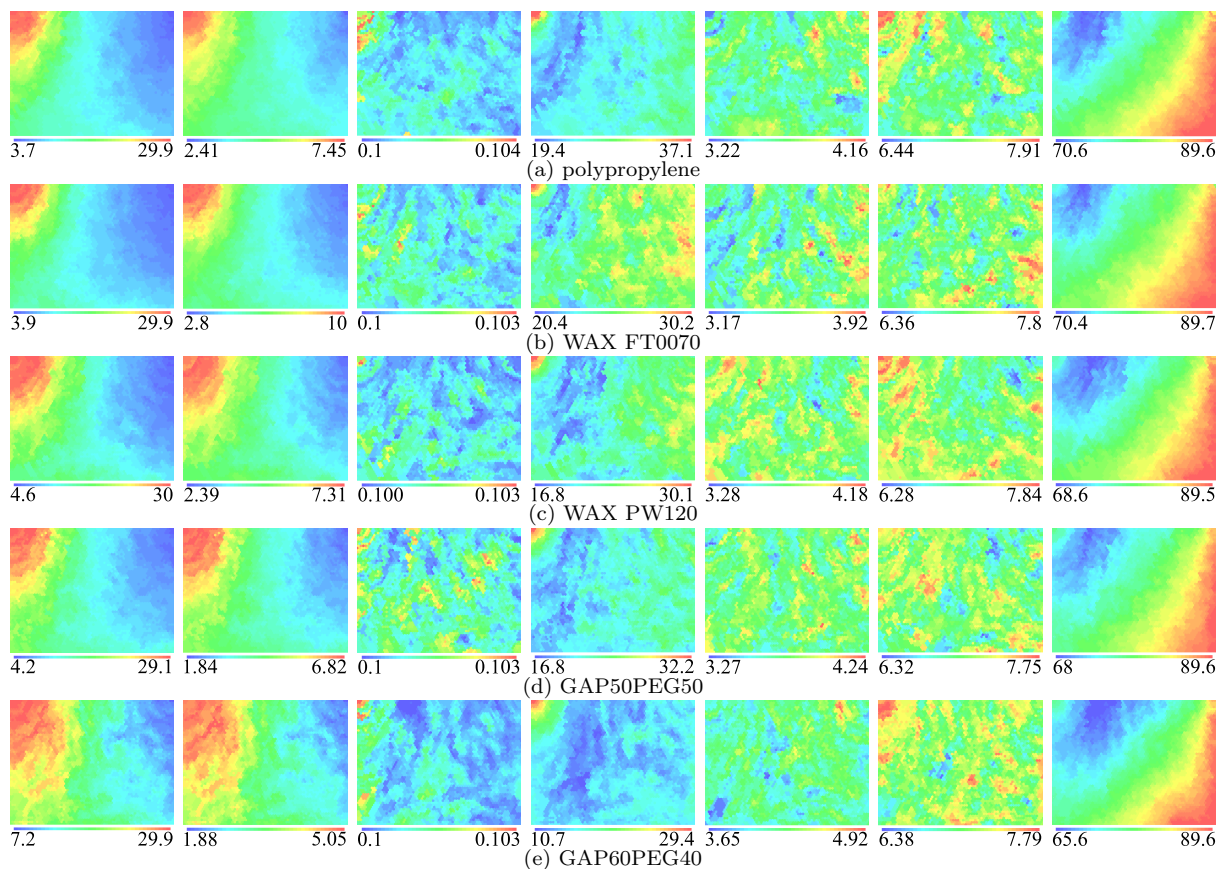
Figure 5: SOMs colored by the design variables. The color range is set to be the max/min values in nondominated solutions. The column means dv1, dv2, $\cdots$, and dv7 from the left.

4.2.2 Behavior of Design Variables to be Nondominated Solutions

Figure 4 reveals the behavior of each design variable in the design space with the defined wide range which is physically available in order to become the nondominated solutions.

All nondominated solutions have higher dv1 than the lower bound of dv1 defined in Table 1. This fact suggests that the minimum initial mass flow of oxidizer is necessary in order to attain to the lower thermosphere(altitude of 90[km]). The mass flow of oxidizer $\dot{m}_{\mathrm{oxi}}(t)$ affects the structural weight because of the increase of the filling pressure of oxidizer tank and the pressure of the combustion chamber $P_{\mathrm{cc}}(t)$. Thereupon, the initial mass flow of oxidizer $\dot{m}_{\mathrm{oxi}}(0)$(dv1) is essential in order to improve the initial gross weight $M_{\mathrm{tot}}(0)$(obj3).

The value of dv2 does not have both high and low. As the minimum fuel length is necessary in order to attain to the lower thermosphere(altitude of 90[km]), dv2 does not have low. On the other hand, as it is considerable that the fuel length L_{fuel}(dv2) does not affect strongly on the maximization of the down range R_d and the duration time T_d

13

rather than the initial mass flow of oxidizer $\dot{m}_{\mathrm{oxi}}(0)$(dv1), the fuel length L_{fuel}(dv2) does not have high value.

The value of dv3 is roughly constant. This fact indicates that there is the optimum initial radius of port $r_{\mathrm{port}}(0)$(dv3), which might be determined by the combustion mode and the swirl intensity. However, when the initial radius of port $r_{\mathrm{port}}(0)$(dv3) is compared among the fuels in Fig. 4, there is no diversity of the value regarding dv3. It reveals that the initial radius of port does not depend on the fuels among the present five fuels. The influence of oxidizer-flow mode is an assignment because of the low-fidelity evaluation model in the present study.

The value of dv4 is in the narrow region of the design space. However, the combustion time t_{burn}(dv4) becomes high when the initial gross weight $M_{\mathrm{tot}}(0)$(obj3) is high. That is, the combustion time t_{burn}(dv4) has identical behavior of the initial radius of port $r_{\mathrm{port}}(0)$(dv3) except the design space where it directly affects on the initial gross weight $M_{\mathrm{tot}}(0)$(obj3) (note that a variable directly affects when degrees of coloring transition between two SOMs are similar(for example, upper left region between obj3 on Fig. 3 and dv4 on Fig. 4). On the other hand, it assumes that a variable indirectly affects when degrees of coloring transition between two SOMs are not similar(for example, upper left region between obj3 on Fig. 3 and dv1 on Fig. 4)). However, WAX fuels, especially FT0070 obtains the high value of combustion time t_{burn}(dv4), it does not depend on the initial gross weight $M_{\mathrm{tot}}(0)$ shown in Fig. 5(b). Since the both of the density ρ_{fuel} and the regression rate $\dot{r}_{\mathrm{port}}(t)$ of FT0070 is low, combustion time t_{burn} consequently becomes long. That is, combustion time t_{burn}(dv4) is a sensitive design variable for the characteristics of the fuels.

The value of dv5 has low value. The high value of the initial pressure in combustion chamber $P_{\mathrm{cc}}(0)$(dv5) fundamentally gives high thrust. As it is expected that the structural requirement is not fulfilled due to high pressure, the structural fulfillment should be confirmed by the parametric study regarding the structural safety factor. In addition, the time fluctuation regarding the pressure in combustion chamber $P_{\mathrm{cc}}(t)$ should be observed in the next-step design problem.

The value of dv6 has the coloring pattern in a muddle which is similar to that of dv5, although there is the difference of color. Since the aperture ratio of nozzle ϵ(dv6) becomes high in order to keep the high thrust, ϵ(dv6) indirectly give the effect on the objective functions. In fact, the high value of dv6 is on the upper left of SOM, which is the region to become high objective functions. However, Fig. 5 indicates that WAX FT0070 and GAP50PEG50 do not augment the initial gross weight $M_{\mathrm{tot}}(0)$(obj3) even when the aperture ratio of nozzle ϵ(dv6) becomes high. The augmentation of combustion time does not exactly join with the increase of the volume of the solid fuels because the regression rate $\dot{r}_{\mathrm{port}}(t)$ is low regarding both of this two fuels. The initial gross weight $M_{\mathrm{tot}}(0)$ is not consequently increased. The aperture ratio of nozzle ϵ(dv6), as well as combustion time t_{burn}(dv4), is a sensitive design variable for the characteristics of fuels.

The coloring pattern of SOM by dv7 is similar to that by obj1. As the vertical launch

14

would be implemented when the elevation at launch time $\phi(0)(dv7)$ becomes high, it is easily understandable that the down range $R_d(obj1)$ is low. The definition of the next-step design problem will be discussed by all designers using the above design information.

4.2.3 Influence of Design Variables on Objective Functions

Figure 5 reveals the influence direction of the design variables for the objective functions. And also the correlations among the design variables is shown when the SOM's coloration pattern is compared between Figs. 3 and 5.

In the first place, the influence of each design variable on the maximization of the down range $R_d(obj1)$ will be summarized. The high-value region of dv1 is in concord with the high-value region of obj1. Since the high value of the initial mass flow of oxidizer $\dot{m}_{\mathrm{oxi}}(0)(dv1)$ increases thrust, the down range $R_d(obj1)$ is sensitive. The high-value region of dv2 is also in concord with the high-value region of obj1. The coloration pattern on SOM regarding dv2 is extremely similar to that regarding dv1. Fuel length $L_{\mathrm{fuel}}(dv2)$ is one of the constitutional elements for the mass flow of the fuel $\dot{m}_{\mathrm{fuel}}(t)$, that is, the mixture ratio between liquid oxidizer and solid fuel $O/F(t)$ strongly has the influence of $L_{\mathrm{fuel}}(dv2)$. As the mixture ratio $O/F(t)$ is essential for the performance of hybrid rocket, the implication of $O/F(t)$ for the down range $R_d(obj1)$ also shows its significance. As the coloration pattern on SOM regarding dv3 is not similar to that regarding obj1, dv3 does not give effects on the optimization of obj1. The initial radius of port $r_{\mathrm{port}}(0)(dv3)$ is not essential for the optimization of the down range $R_d(obj1)$ whenever the value of $r_{\mathrm{port}}(0)(dv3)$ stays in the range to become nondominated solutions. High value of dv4 achieves optimizing obj1. However, the down range can be high even when combustion time $t_{\mathrm{burn}}(dv4)$ is less than the threshold(roughly 27[sec]). This is because the region on the upper left SOM is different coloration patterns between obj1 and dv4 and the transformation of color on SOM of dv4 is sharp. Since the coloration pattern of SOM regarding dv5 is not in concord with that regarding obj1, there is no direct influence on obj1. As the pressure in combustion chamber $P_{\mathrm{cc}}(t)$ has the constraints regarding the structure mode and the safety factor, the initial pressure in combustion chamber $P_{\mathrm{cc}}(0)(dv5)$ would not have the flexibility to affect on the down range $R_d(obj1)$. Therefore, the sensitivities of the structure mode and the safety factor should be investigated. As the coloration pattern of SOM regarding dv6 is similar to that regarding dv5, it reveals that there is also no direct influence on obj1. Although the high value of dv6 tends to optimize obj1, dv6 is not essential. The aperture ratio of nozzle $\epsilon(dv6)$ is not uniquely determined for the down range $R_d(obj1)$ and the other objective functions because the optimum aperture ratio of nozzle is fluctuated by the pressures in combustion chamber and flight altitude in order to be optimum expansion. Therefore, the aperture ratio of nozzle $\epsilon(dv6)$ does not directly have the influence on the down range R_d. Although the value of dv7 should be low in order to optimize obj1, it should not be too low. Although the down range $R_d(obj1)$ increases when the elevation $\phi(dv7)$ is low, the maximum attainable altitude

decreases due to the projectile motion which is the assumed flight sequence. Therefore, multi-time ignition is essential in order that the down range is increased whereas the maximum attainable altitude keeps high.

In the second place, the influence on the maximization of the duration time T_d(obj2) will be summarized. The coloration pattern of all of the SOMs regarding the design variables is different from that of SOM regarding obj2. This difference depends on the manageable objective function due to its upper limitation. The maximization of obj2 is connotatively accompanied the maximization of obj1. When the influence of the design variables on obj2 will be minutely investigated, the local nondominated solutions on the convex surface in Fig. 2(c) should be extracted in order that mining is separately performed for them.

In the third place, the influence on the minimization of the initial gross weight $M_{tot}(0)$(obj3) will be summarized. As the coloration pattern of SOM's right hand side regarding dv1 is in concord with that regarding obj3. This fact reveals that dv1-reduction is the necessary condition to minimize obj3. Since the volume of the installed oxidizer decreases when the initial mass flow of oxidizer $\dot{m}_{oxi}(0)$(dv1) is reduced, the initial gross weight $M_{tot}(0)$(obj3) is consequently reduced. As the initial mass flow of oxidizer $\dot{m}_{oxi}(0)$(dv1) gives effect on the maximization of the down range R_d(obj1), this design variable $\dot{m}_{oxi}(0)$(dv1) covers the essential role in the present study. The coloration pattern of SOM regarding dv2 is similar to that regarding dv1. The initial gross weight $M_{tot}(0)$(obj3) can be reasonably reduced when the fuel length L_{fuel}(dv2) shortens. The colored SOMs show that the values of dv3, dv4, dv5, and dv6 are not directly effective on obj3. Although the high value of dv7 is a necessary condition to minimize obj3, the optimum direction is different between dv7 and obj3. Therefore, it is considerable that dv1 and dv2 directly give effects on obj3. When the elevation at launch time $\phi(0)$(dv7) becomes high(in the vicinity of 90[deg]), the necessary volume of the fuel can be held down because the flight distance from the ground to the lower thermosphere(altitude of 90[km]) shortens. The initial gross weight $M_{tot}(0)$(obj3) consequently becomes low.

4.3 Implication of Difference among Fuels

4.3.1 Knowledge Acquired from Plots of Nondominated Solutions

Although there reveals no drastic transformation of the objective functions by the fuels, the implication of each fuel will be compared by using Fig. 2. The performance in the case using polypropylene will be set as a criterion. The extension of the duration time T_d(obj2) cannot be achieved by all of the other fuels because the limitation is already reached by using polypropylene. The reduction of the initial gross weight $M_{tot}(0)$(obj3) can be achieved by any fuel. When WAX-type fuels are used, 17% of the initial gross weight $M_{tot}(0)$ is reduced. There is no specific difference between WAX FT0070 and PW120 regarding the influence on the initial gross weight. When the compounds between GAP and PEG are used, maximum 40% of the initial gross weight $M_{tot}(0)$ is reduced. GAP60PEG40 is better performance than GAP50PEG50 regarding the reduction of the

initial gross weight $M_{\text{tot}}(0)$(obj3). The performance for the extension of the down range R_d(obj1) is identical between polypropylene and WAX-type fuels. On the other hand, the compounds between GAP and PEG has the performance of maximum 4%(roughly 10[km]) increase for the down range R_d(obj1). The selection of the compounds between GAP and PEG materializes to hold down the initial gross weight $M_{\text{tot}}(0)$(obj3) and to also augment the down range R_d(obj1).

4.3.2 Knowledge Acquired from SOM

The colored SOMs shown in Figs. 3 and 4 reveal the qualitative correlation among the objective functions and the difference of the behavior in the design space regarding the design variables. Figure 3 shows that there is no significant difference among the fuels regarding the correlations among the objective functions. On the other hand, Fig. 4 reveals that WAX FT0070 and GAP60PEG40 have meaningful distinctions for the behavior of design variables.

Regarding WAX FT0070, fuel length L_{fuel}(dv2) is higher and the initial pressure in combustion chamber $P_{\text{cc}}(0)$(dv5) is lower than that of the other fuels. Since the regression rate $\dot{r}_{\text{port}}(t)$ of WAX FT0070 is low shown in Fig. 1, L_{fuel} should be high in order to secure the mass flow of fuel $\dot{m}_{\text{fuel}}(t)$ in eq. (1). And also, as $\dot{m}_{\text{fuel}}(t)$ becomes low when $\dot{r}_{\text{port}}(t)$ of WAX FT0070 is low, the internal pressure of combustion chamber $P_{\text{cc}}(t)$ becomes low. $P_{\text{cc}}(t)$ is described as follows,

$$P_{\text{cc}}(t) = \frac{(\dot{m}_{\text{oxi}}(t) + \dot{m}_{\text{fuel}}(t)) \cdot c^*(t)}{A_{\text{throat}}}, \tag{3}$$

where, $c^*(t)$ and A_{throat} respectively represents characteristic exhaust velocity and the area at nozzle throat.

Regarding GAP60PEG40, the combustion time t_{burn}(dv4) is lower and the initial pressure in combustion chamber $P_{\text{cc}}(0)$(dv5) is higher than that of the other fuels. As the regression rate $\dot{r}_{\text{port}}(t)$ of GAP60PEG40 is high shown in Fig. 1, t_{burn} can be shortened under the condition of equal fuel volume. And also, as the mass flow of fuel $\dot{m}_{\text{fuel}}(t)$ is high because $\dot{r}_{\text{port}}(t)$ of GAP60PEG40 is high, $P_{\text{cc}}(t)$ becomes high in eq. (3). Although $\dot{m}_{\text{oxi}}(0)$(dv1) has larger region of high value and does not have lower value, this result does not depend on a physical difference because $\dot{m}_{\text{oxi}}(t)$ is determined by the balance among $\dot{r}_{\text{port}}(t)$, a_{fuel}, and n_{fuel} in eq. (2). $\dot{m}_{\text{oxi}}(t)$ as a whole is high due to the high values of $\dot{r}_{\text{port}}(t)$ and a_{fuel}, and the low value of n_{fuel}.

Note that the estimation model of the regression rate shown in eq. (2) is experimentally derived. The exact values of the experimental data at under 200 [kg/m^2/sec] of oxidizer mass flux $G_{\text{oxi}}(t)$ regarding two WAX-type fuels are used for eq. (2). That is, the values of the regression rate for two WAX-type fuels at over 200 [kg/m^2/sec] are extrapolated by eq. (2). The data obtained by the latest experiments at higher $G_{\text{oxi}}(t)$ reveals that WAX-type fuels have augmentative regression rate compared with the data shown in Fig. 1.

Thereupon, the experimental model eq. (2) should be modified. On the other hand, the obtained results in the present study reveal the sensitive design variables for the fuels and their behaviors for the regression rate. This knowledge is generally essential.

5 CONCLUSIONS

The next-generation single-stage launch vehicle with the hybrid rocket engine of solid fuel and liquid oxidizer in place of the present pure solid-fuel rockets has been conceptually designed in view of the implication of fuels by using design informatics in order to contribute to the low cost launch vehicle system and efficient space scientific observation. The objective functions as the design requirements in the design problem is the maximization of the down range and the duration time in the lower thermosphere as well as the minimization of initial gross weight. A hybrid evolutionary computation between the differential evolution and the genetic algorithm is employed for the efficient exploration in the design space so as to construct polished hypothetical database for data mining. A self-organizing map is used in order to structurize and visualize the design space. Moreover, the influence of difference of solid fuels for design information has been discussed.

Consequently, the design information has been revealed regarding the tradeoffs among the objective functions, the behavior of the design variables in the design space, and the correlations between the objective functions and the design variables. Moreover, the comparison of the implication of five fuels reveals that the compounds between 60% of glycidyl azide polymer and 40% of polyethylene glycol is better performance. These results indicates that the ascendancy of multi-time ignition as the advantage of hybrid rocket will be quantitatively shown in the third-step conceptual design in the future.

ACKNOWLEDMENT

REFERENCES

[1] Karabeyoglu, M. A. Advanced hybrid rockets for future space launch. In *Proceedings on 5th European Conference for Aeronautics and Space Sciences*. EUCASS, (2013).

[2] Simurda, L., Zilliac, G., and Zaseck, C. High performance hybrid propulsion system for small satellites. In *AIAA Paper 2013-3635*. AIAA, (2013).

[3] Saraniero, M. A., Caveny, L. H., and Summerfield, M. Restart transients of hybrid rocket engines. *Journal of Spacecraft and Rockets* **10**(3), 215–217 (1973).

[4] Karabeyoglu, M. A., Altman, D., and Cantwell, B. J. Combustion of liquefying hybrid propellants: Part 1, general theory. *Journal of Propulsion and Power* **18**(3), 610–620 (2002).

[5] Arias-Montano, A., Coello, C. A. C., and Mezura-Montes, E. Multiobjective evolutionary algorithms in aeronautical and aerospace engineering. *IEEE Transactions on Evolutionary Computation* **16**(5), 662–694 (2012).

[6] Chiba, K., Makino, Y., and Takatoya, T. Design-informatics approach for intimate configuration of silent supersonic technology demonstrator. *Journal of Aircraft* **49**(5), 1200–1211 (2012).

[7] Chiba, K., Kanazaki, M., Nakamiya, M., Kitagawa, K., and Shimada, T. Conceptual design of single-stage launch vehicle with hybrid rocket engine for scientific observation using design informatics. *Journal of Space Engineering* **6**(1), 15–27 (2013).

[8] Keane, A. J. Statistical improvement criteria for use in multiobjective design optimization. *AIAA Journal* **44**(4), 879–891 (2006).

[9] Jeong, S., Murayama, M., and Yamamoto, K. Efficient optimization design method using kriging model. *Journal of Aircraft* **42**(2), 413–420 (2005).

[10] Chiba, K. Evolutionary hybrid computation in view of design information by data mining. In *Proceedings on IEEE Congress on Evolutionary Computation*, 3387–3394. IEEE, (2013).

[11] Kohonen, T. *Self-Organizing Maps*. Springer, Berlin, Heidelberg, (1995).

[12] Deboeck, G. and Kohonen, T. *Visual Explorations in Finance with Self-Organizing Maps*. London, Springer Finance, (1998).

[13] Chiba, K. and Obayashi, S. Knowledge discovery in aerodynamic design space for flyback-booster wing using data mining. *Journal of Spacecraft and Rockets* **45**(5), 975–987 (2008).

[14] Arthur, W. The emerging conceptual framework of evolutionary developmental biology. *Nature* **415**(6873), 757–764 (2002).

[15] Oyama, A., Obayashi, S., and Nakamura, T. Real-coded adaptive range genetic algorithm applied to transonic wing optimization. *Applied Soft Computing* **1**(3), 179–187 (2001).

[16] Deb, K., Pratap, A., Agarwal, S., and Meyarivan, T. A fast and elitist multiobjective genetic algorithm: Nsga-ii. *IEEE Transactions on Evolutionary Computation* **6**(2), 182–197 (2002).

[17] Fonseca, C. M. and Fleming, P. J. Genetic algorithms for multiobjective optimization: Formulation, discussion and generalization. In *Proceedings of the Fifth International Conference on Genetic Algorithms*, 416–423. Morgan Kaufmann, (1993).

[18] Baker, J. E. Adaptive selection methods for genetic algorithms. In *Proceedings of the International Conference on Genetic Algorithms and their Applications*, 101–111. Lawrence Erlbaum Associates, (1985).

[19] Takahashi, M. and Kita, H. A crossover operator using independent component analysis for real-coded genetic algorithms. In *Proceedings of IEEE Congress on Evolutionary Computation 2001*, 643–649. IEEE, (2001).

[20] Hervas-Martinez, C., Ortiz-Bayer, D., and Garcia-Pedrajas, N. Theoretical analysis of the confidence interval based crossover for real-coded genetic algorithms. In *The 7th International Conference on Parallel Problem Solving from Nature, LNCS 2439*, 153–161 (Springer-Verlag, Berlin Heidelberg, 2002).

[21] Robic, T. and Filipic, B. Demo: Differential evolution for multiobjective optimization. In *The 3rd International Conference on Evolutionary Multi-Criterion Optimization, LNCS 3410*, 520–533 (Splinger-Verlag, Guanajuato, Mexico, 2005).

[22] Sasaki, D. and Obayashi, S. Efficient search for trade-offs by adaptive range multiobjective genetic algorithms. *Journal of Aerospace Computing, Information, and Communication* **2**(1), 44–64 (2005).

[23] Kosugi, Y., Oyama, A., Fujii, K., and Kanazaki, M. Multidisciplinary and multiobjective design exploration methodology for conceptual design of a hybrid rocket. In *AIAA Paper 2011-1634*. AIAA, (2011).

[24] Gordon, S. and McBride, B. J. Computer program for calculation of complex chemical equilibrium compositions and applications i. analysis. In *NASA Reference Publication RP-1311*. NASA, (1994).

[25] Hirata, K., Sezaki, C., Yuasa, S., Shiraishi, N., and Sakurai, T. Fuel regression rate behavior for various fuels in swirling-oxidizer-flow-type hybrid rocket engines. In *AIAA Paper 2011-5677*. AIAA, (2011).

[26] Yuasa, S., Shiraishi, N., and Hirata, K. Controlling parameters for fuel regression rate of swirling-oxidizer-flow-type hybrid rocket engine. In *AIAA Paper 2012-4106*. AIAA, (2012).